Anisotropic dynamical coupling for propagating collective modes in a two-dimensional magnonic crystal consisting of interacting squared nanodots

S. Tacchi,[1] M. Madami,[1] G. Gubbiotti,[1] G. Carlotti,[1,2] H. Tanigawa,[3] T. Ono,[3] and M. P. Kostylev[4]
[1]*CNISM, Unità di Perugia, Dipartimento di Fisica, Università di Perugia, Via A. Pascoli, I-06123 Perugia, Italy*
[2]*Centro S3, CNR-Istituto di Nanoscienze, Via Campi 213A, I-41125 Modena, Italy*
[3]*Institute for Chemical Research, Kyoto University, Uji, Kyoto 611-0011, Japan*
[4]*School of Physics M013, University of Western Australia, 35 Stirling Hwy, 6009 Western Australia, Australia*
(Received 13 April 2010; published 2 July 2010)

Collective spin excitations in a planar array of interacting submicron magnetic squared dots have been studied by the Brillouin light-scattering technique. The dispersion curves of collective spin modes are characterized by periodical oscillations determined by the width of the artificial Brillouin zone. Because of the uniaxial symmetry introduced by the application of an external magnetic field H_0, the dynamical coupling and the frequency dispersion of collective modes are different when the wave vector is perpendicular or parallel to H_0. An analytical model has been exploited to calculate the dispersion of collective spin modes by numerically solving eigenvalue/eigenfunction problem for a band matrix which originates from linearized Landau-Lifshitz magnetic torque equation. A very good agreement between calculation and experiment was found. In addition, a micromagnetic approach has been exploited to achieve an independent evaluation of the collective modes frequency and a visualization of their spatial profile on a limited (3×3) array of dots.

DOI: 10.1103/PhysRevB.82.024401 PACS number(s): 75.30.Ds, 78.35.+c, 75.78.Cd, 75.75.Jn

I. INTRODUCTION

Spin dynamics in ordered arrays of interacting nanomagnets has recently received increased attention, in view of the emerging research field of *magnonics* whose aim is the realization of artificial structures (called *magnonic crystals*) where propagating spin waves are used to carry and process information.[1,2] In this context, plane ordered arrays of interacting elements offer the opportunity to realize magnonic crystals where it is possible to control the spin-wave propagation by exploiting the pattern geometry (plane magnonic crystals). In arrays of periodically spaced nanomagnets, in fact, the dipolar interaction couples resonances of individual elements leading to the formation of collective modes in the form of Bloch waves.[3–10] As for any periodical medium, a Bloch wave number describes the wave process and it is unambiguously defined in the first Brillouin zone (BZ) of the artificial crystal lattice. Furthermore, the dispersion of the waves is characterized by the presence of allowed magnonic states and ranges of forbidden frequencies (band gaps).

In most of previous works cited above, the magnonic band gaps were experimentally observed by Brillouin light scattering (BLS) in one-dimensional (1D) arrays consisting of longitudinally magnetized nanostripes. It was shown that these structures support propagation of Bloch waves at any angle between the wave vector and the long axis of the stripes but the magnonic gaps are partial, as shown in Ref. 7: allowed magnonic bands for collective mode propagation along the stripes overlap with magnonic gaps for propagation in the direction of the array periodicity.

Similar to the case of 1D structures, also two-dimensional (2D) artificial magnonic crystals can be fabricated in the form of ordered arrays of closely packed magnetic dots coupled by dipolar interaction. The first attempts to prove the effect of dynamical coupling on the spin excitations of 2D arrays of dots were made by studying the effect of interdot distance on the magnetic modes frequency.[11–13] BLS experiments carried out on squared arrays of micron-size circular NiFe dots revealed the presence of a fourfold anisotropy, attributed to the dynamic magnetic dipole interaction between the dots at small interelement distances. However, in these pioneering experiments neither dispersive modes nor bands formation were detected. Furthermore, no quantitative description of the interplay between static and dynamic stray fields was provided. More recently, experimental studies in 2D array of interacting nanoelements (excited by the quasiuniform field of a coplanar transmission line) were reported by time-resolved Kerr microscopy[14,15] and ferromagnetic resonance[16] but no experimental evidence of frequency dispersion and propagating character of such modes could be given because with the two techniques above it is not possible to sweep the wave vector of measured excitations.

In this work we investigate the frequency dispersion and the propagation characteristics of collective spin excitations in a dense 2D array of submicrometric size square dots by BLS. One of the important advantages of our technique is its capability to separate the dynamic coupling of elements from their static coupling. This is achieved by observing variation in the BLS response for different values and directions of the exchanged in-plane wave vector at a fixed external field. A strong dependence of dynamical dipole coupling on the direction of collective mode propagation is observed and discussed in terms of the symmetry breaking imposed by the application of the external dc magnetic field. To achieve a quantitative interpretation of the experimental data, a calculation of collective modes is performed by numerically solving an eigenvalue/eigenfunction problem for a band matrix which originates from the linearized Landau-Lifshitz magnetic torque equation. In addition, a micromagnetic approach is exploited to carry out an independent estimation of eigenfrequencies of the collective modes and to visualize of their spatial profiles on a limited (3×3) array of dots.

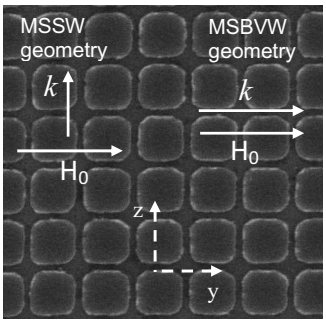

FIG. 1. SEM image of the array of squared dots. BLS spectra were measured in two scattering geometries corresponding to the different orientations of the external magnetic field H_0 with respect to the direction of the exchanged wave vector k. The MSSW geometry is for k perpendicular to H_0 while the MSBVW one corresponds to k parallel to H_0.

II. EXPERIMENT AND MICROMAGNETIC MODELING

A large array (1×1 mm^2) of $L=30$-nm-thick square dots, having lateral size $w=450$ nm and interdot spacing $\Delta=70$ nm (period $a=w+\Delta=520$ nm; first Brillouin-zone boundary $k_{BZ}=\pi/a=0.6\times10^5$ rad/cm) has been fabricated on thermally oxidized Si substrate by means of e-beam lithography, electron-gun deposition and lift-off process. A Scanning electron microscopy (SEM) image of the array is shown in Fig. 1.

Brillouin light-scattering experiments were performed in the backscattering configuration, using the $\lambda=532$ nm green light of a single-mode diode-pumped solid-state laser and a Sandercock-type (3+3)-pass tandem Fabry-Perot interferometer. To study the dispersion of propagating collective modes, BLS spectra were measured at different incidence angles of light θ in the range between 0° and 70°. This corresponds to variation in the absolute value of the in-plane transferred wave vector, $k=2(2\pi/\lambda)\sin\theta$, in the range between 0 and 2.2×10^5 rad/cm.

Measurements were carried out in two different configurations with the external magnetic field $H_0=1.5$ kOe applied in the sample plane along the y axis, i.e., along one of the element edges: (a) magnetostatic surface waves geometry (MSSW), also known as Voigt geometry, where the transferred wave vector k is perpendicular to H_0. (b) Magnetostatic backward volume waves (MSBVW) geometry where the transferred wave vector k is parallel to H_0.

Micromagnetic simulations have been performed by using the OOMMF package.[17] Due to the time-consuming characteristics of such simulations, we restricted our analysis to a finite array consisting of 3×3 squared dots. The procedure we used to simulate the eigenmodes frequency and spatial profile is already described in Refs. 9 and 18 and it is shortly recalled here. The first step of the process consists in calculating the static magnetization configuration for an in-plane applied dc field H_0. The obtained magnetic ground state is then used as the initial magnetization configuration for the dynamical calculation. Retaining the value of the external dc uniform field, which is constant in time, the system is excited by an out-of-plane Gaussian pulse, with a full width at half maximum of 1 ps and an amplitude of 10 Oe. To investigate the efficiency of the dynamical coupling in excited magnetic normal modes of adjacent dots,[19] we apply this field pulse only to the central dot of the 3×3 array. After the field pulse is applied the system is left free to evolve following the Landau-Lifshitz equation of motion with a damping factor artificially set to a low value $\alpha=0.0001$. Magnetization ring down in each cell for every dot of the array is recorded. A temporal Fourier analysis of these data is carried out to produce the local power spectra of the magnetization. A surface plot of the imaginary part of the Fourier coefficients for each eigenfrequency provides the two-dimensional profile of the corresponding eigenmode. The magnetic parameters used in the micromagnetic calculations are extracted from the fitting of the surface and first perpendicular standing spin wave of the 30-nm-thick continuous NiFe film, as shown in Fig. 2. The parameters extracted from the best-fit procedure and used for the calculation are the following: saturation magnetization $4\pi M_0=10.3$ kOe, gyromagnetic constant $\gamma=2.93$ MHz/Oe and exchange constant $A=1.0\times10^{-6}$ erg/cm.

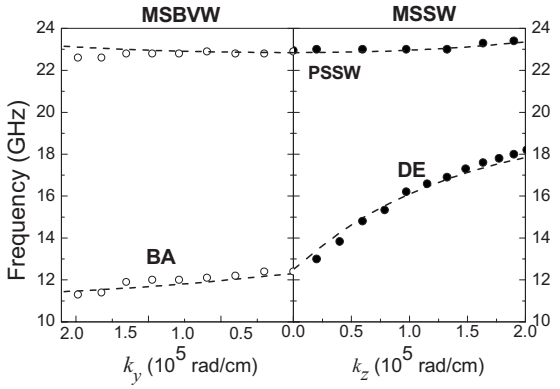

FIG. 2. Measured (points) and calculated (dashed curves) frequency dispersion for the continuous (unpatterned) 30-nm-thick NiFe film. The so-called DE (full points) was measured in the MSSW configuration while the BA (open circles) was measured in the MSBVW configuration. The first perpendicular standing spin wave (full and open circles at about 23 GHz) was detected in both configurations.

III. THEORY

To calculate eigenfrequencies of collective modes we use a Fourier-space approach. It is an extension on the 2D case of the original method recently implemented for the quasi-1D magnonic crystal.[20] Referring to the reference frame defined in Fig. 1, we start with the linearized Landau-Lifschitz equation

$$-i\omega\mathbf{m}(\mathbf{r}) = -\gamma\{\mathbf{M}(\mathbf{r})\times[\mathbf{h}_{ex}(\mathbf{r})+\mathbf{h}_d(\mathbf{r})]+\mathbf{H}_0(\mathbf{r})\times\mathbf{m}(\mathbf{r})\}, \tag{1}$$

where $\mathbf{m}(\mathbf{r})$ is the dynamic magnetization, $\mathbf{r}$ is the radius vector, $\mathbf{h}_{ex}(\mathbf{r})$ and $\mathbf{h}_d(\mathbf{r})$ are the dynamic exchange and dipole fields, respectively, $H_0(\mathbf{r})=H_0(\mathbf{r})\mathbf{e}_y$ is the static internal field of the dots, and $\mathbf{M}(\mathbf{r})$ is the static magnetization. Following

the approach in Refs. 21 and 22, we neglect inhomogeneity of the static magnetization inside the elements. Thus

$$\mathbf{M}(\mathbf{r}) = \begin{cases} M_0\mathbf{e}_y & \text{inside the dots} \\ 0 & \text{in the gaps between dots.} \end{cases}$$

The effective exchange field is defined as follows:

$$\mathbf{h}_{ex}(\mathbf{r}) = \alpha\nabla^2\mathbf{m}(\mathbf{r}). \tag{2}$$

We also neglect the inhomogeneity of distribution of dynamic magnetization and of its dipole and exchange field across the dot thickness, i.e., along the axis x. For elements with a small aspect ratio $L/w \ll 1$ this approximation is appropriate as shown in multiple previous studies.[6,22,23]

As the system is periodical in both directions, we use the Bloch-Floquet theorem to write down a solution for $\mathbf{m}(\boldsymbol{\rho}) = \mathbf{m}(y,z)$ in the form of plane Bloch waves: $\mathbf{m}(\boldsymbol{\rho}) = \tilde{\mathbf{m}}(\boldsymbol{\rho})\exp(i\mathbf{k}_B\boldsymbol{\rho})$, where $\tilde{\mathbf{m}}(\boldsymbol{\rho}) = \tilde{\mathbf{m}}(\boldsymbol{\rho}+\mathbf{a})$ is a periodic function, $\mathbf{a}$ is the lattice vector for the 2D quasicrystal, and $\mathbf{k}_B$ is the Bloch vector of the collective mode. We then expand all periodic quantities into Fourier series and obtain the following relations:

$$\mathbf{m}(y,z) = \sum_{j=-\infty}^{\infty}\sum_{l=-\infty}^{\infty}\mathbf{m}_{j,l}\exp(ik_{yj}y + ik_{zl}z) \times\exp(ik_{By}y + ik_{Bz}z),$$

$$\mathbf{h}_{ex}(y,z) = -\alpha\sum_{j=-\infty}^{\infty}\sum_{l=-\infty}^{\infty}K_{j,l}^2\mathbf{m}_{j,l}\exp(ik_{yj}y + ik_{zl}z) \times\exp(ik_{By}y + ik_{Bz}z),$$

$$\mathbf{h}_d(y,z) = \sum_{j=-\infty}^{\infty}\sum_{l=-\infty}^{\infty}\hat{P}(K_{j,l})\mathbf{m}_{j,l}\exp(ik_{yj}y + ik_{zl}z) \times\exp(ik_{By}y + ik_{Bz}z). \tag{3}$$

In these expressions $k_{yj}=2\pi j/a$, $k_{zl}=2\pi l/a$, $j,l=\ldots,-1,0,1,\ldots$, and $K_{j,l}^2=(k_{yj}+k_{By})^2+(k_{zl}+k_{Bz})^2$, $\hat{P}(|q|)$ is the dynamic dipole-field tensor with components: $P_{zz}(|q|) = -F(|q|)\sin^2[\varphi(q)]$, $P_{xx}(|q|)=F(|q|)-1$, $\sin[\varphi(q)]=q_z/|q|$, and $\mathbf{q}$ is some "dummy" wave vector. The function $F(q)$ is defined, as follows: $F(q)=1-[1-\exp(-|qL|)]/|qL|$.[24] It represents the Fourier *integral* transform

$$F(q) = \frac{1}{2\pi}\int_{-\infty}^{\infty}G(s)\exp(-iqs)ds \tag{4}$$

of the thickness-averaged Green's function of dynamic dipole field[23]

$$G(s) = (1/L)\ln[s^2/(s^2+L^2)] \tag{5}$$

(see Ref. 25 for details).

Substituting Eqs. (3) into Eq. (1) results in a system of coupled equations as follows:

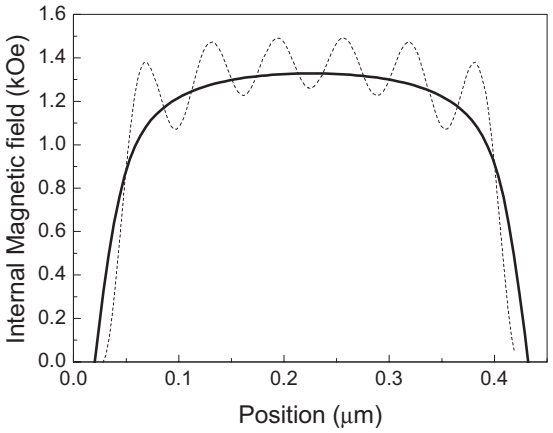

FIG. 3. Section of the static internal magnetic field of the dots along the field direction. The section is taken at the center of the dot. Thick solid line: OOMMF simulation for the central dot of a 3×3 array of dots. Thin black dashed line: truncated Fourier-series solution in Eq. (7). Note that the approximate calculation using the formula (7) gives an internal field which is homogeneous across dots in the direction perpendicular to the applied field.

$$i(\omega/\gamma)\mathbf{m}_{n,m,\boldsymbol{\kappa}_B} = \sum_{n',m'=-\infty}^{\infty}\{\mathbf{M}_{n-n',m-m'}[-\alpha|\mathbf{k}_{n',m'}+\mathbf{k}_B|^2\mathbf{m}_{n',m',\boldsymbol{\kappa}_B} + \hat{P}(|\mathbf{k}_{n',m'}+\mathbf{k}_B|)\mathbf{m}_{n',m',\boldsymbol{\kappa}_B}] + \mathbf{H}_{0n-n',m-m'}\times\mathbf{m}_{n',m',\boldsymbol{\kappa}_B}\}, \tag{6}$$

where $\mathbf{M}_{j,l}$ is the Fourier-series transform of Eq. (2). The Fourier-series transform $\mathbf{H}_{0j,l}$ of the internal static field and $\mathbf{H}_0$ is related to $\mathbf{M}_{j,l}$ by the same dipole-field function (4)

$$\mathbf{H}_{0j,l} = -F(|k_{j,l}|)\cos[\varphi(k_{j,l})]\mathbf{M}_{j,l}. \tag{7}$$

The homogeneous infinite system of algebraic Eq. (6) represents an eigenvalue and eigenvector problem for a matrix of coefficients of the system. It allows numerical solution. The eigenvalues are values of $i(\omega/\gamma)$ and the eigenvectors give amplitudes of Fourier harmonics of the collective modes. The square of the modulus of the fundamental harmonics $j=0$, $l=0$ ($\mathbf{m}_{0,0,\boldsymbol{\kappa}_B}$) is proportional to the BLS response seen at the incidence angle $\theta=a\sin[k\lambda/(4\pi)]$.[26] (In this description k is not limited to the first BZ and can span over any point of the reciprocal space). To solve Eq. (6) numerically one has to truncate the series at some values of j and l. In accordance to Ref. 27 the approach of the thickness averaged Green's function (4) and (5) is valid for $|k|L\leq 2$ which gives for the truncation order $|j|,|l|=(w+\Delta)/(\pi L)$. In accordance with this formula in our numerical calculations we took into account harmonics with j and l from -10 to $+10$ (21 harmonics in total). Figure 3 shows the profile of static internal field, defined as the sum of the Zeeman field H_0 and the demagnetizing field, calculated by using both the OOMMF micromagnetic simulation and the above formula [Eq. (7)].

From the figure one sees that the 21-harmonics approximation has good accuracy. The coefficients of the system Eq.

(6) form a matrix containing $(2\times21\times21)\times(2\times21\times21)$ elements. Its 881 eigenvalues for a given value of the Bloch wave number represent array eigenfrequencies. One half of the eigenvalues is positive and one half is negative but having the same absolute values as the positive ones. To compare with experimental data, we performed the following steps: (a) selection of the 20 positive eigenvalues which correspond to the largest BLS responses, according to the discussion above and (b) calculation of the inverse 2D Fourier transform [the first of Eqs. (3)] of the calculated eigenvectors. This gives the eigenmode spatial profiles which allow one identifying these modes.

It is interesting to notice that, due to the relatively weak strength of the dipolar coupling, the collective excitations in the matrix of square dots, whose profiles can be obtained with Eq. (6), can be regarded as formed by the stationary resonances of individual elements (slightly deformed by the dipolar interaction) combined with different phases to form a Bloch wave propagating through the whole pattern. Therefore, for the nomenclature and the labeling of collective modes, we use here the same scheme adopted in previous papers for stationary eigenmodes of non interacting dots, according to their spatial symmetry.[28] For instance, we label as fundamental (F) the mode characterized by the absence of nodes within each dot. Then we distinguish between Damon-Eshbach-type modes, n-DE, characterized by n nodal surfaces nearly parallel to the static magnetization and backwardlike modes, m-BA, with m nodal surfaces nearly perpendicular to the static magnetization. Mixed modes have nodal planes both parallel and perpendicular to the external field and are labeled by the two indexes n and m. Finally, there are end modes localized at the borders of the dots. Analysis of mode profiles reveals that end modes (EMs) can be divided in to DE-like and BA-like EMs depending on the presence of nodal planes in the perpendicular or parallel direction with respect to the external magnetic field. Therefore, if the EM has no nodes we label it EM_F, while in presence of a number m or n of nodes, we will use the labels EM_{nDE} or EM_{mBA}.

IV. RESULTS AND DISCUSSION

A. Comparison between experimental spectra and theory

Figure 4 shows two sequences of BLS spectra, recorded in the MSBVW and MSSW configurations at different values of the incidence angle of light, i.e., different magnitude of the transferred wave number k. Spectra measured in both scattering geometries reveal several peaks in the frequency range between 5 and 18 GHz. First of all we focus our attention on the frequency range above 10 GHz. In the MSSW geometry we found sizeable frequency dispersion for a couple of modes as seen in Fig. 4, right panel. This behavior is different from the case of noninteracting stripes where, as a consequence of lateral confinement, quantized spin wave with nondispersive character have been observed,[29] and it is a clear signature of the formation of propagating collective modes, as discussed in the following. On the contrary, in the MSBVW geometry amplitudes of dispersion for all spin-wave modes are considerably less pronounced (Fig. 4, left panel). From a careful comparison between the measured spectra and the calculated mode frequencies and profiles, we could assign a label to each of the detected modes, as indicated in Fig. 4. In the first BZ (θ and k below about 15° and 0.6×10^5 rad/cm, respectively) the F mode has the largest cross section whatever the experimental configuration. As the value of θ is increased, the most intense peak in BLS spectra moves towards higher order modes, as seen in Fig. 4. In particular, the more intense BLS peaks originate from DE-type (BA-type) collective excitations in the MSSW (MSBVW) scattering geometry respectively. In fact, the light-scattering intensity is proportional to the squared Fourier transform of the dynamic magnetization along the in-plane direction of the wave vector k, as shown in previous investigations of magnetic wires[11] and dots.[30,31] This is also in agreement with a recent theory for the BLS response of thermal collective modes on arrays of dipole coupled stripes.[32]

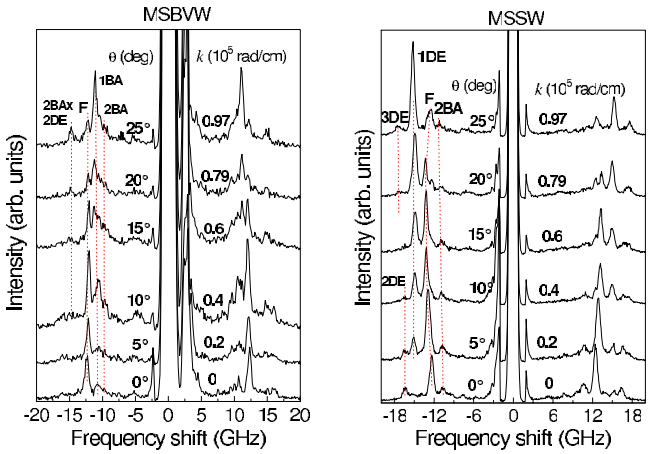

FIG. 4. (Color online) Brillouin spectra recorded in the MSBVW (left panel) and in the MSSW (right panel) configuration, at different value of the incidence angle of light, for a fixed applied magnetic field $H_0=1.5$ kOe.

In Fig. 5 the measured and calculated frequencies are reported as a function of the transferred wave-vector magnitude, for both the MSSW and the MSBVW configuration. The bold portion of curves indicates the most intense peak in the calculation, assuming that its intensity is proportional to the square of the modulus of the fundamental harmonics $\mathbf{m}_{0,0,\kappa_B}$ (see discussion above). It can be seen that the calculation correctly predicts not only the modes frequency, but also their intensity (compare with experimental BLS intensity spectra in Fig. 4), allowing us an unambiguous identification of experimentally measured BLS responses.

One has to note that to obtain this agreement we had to decrease the value of the applied field in the calculation to 1.4 kOe (with respect to the experimental value $H_0=1.5$ kOe). We believe that the approximation of homogeneous distribution of dynamic magnetization across the element thickness and, especially, of the approximation of the homogeneous static magnetization across the element width[22,23] were the reasons which required this small correction of the applied field value. In spite of this, the method of calculation is very efficient and the time of calculation of the whole set of frequencies for a given value of Bloch wave number is about 1 minute.

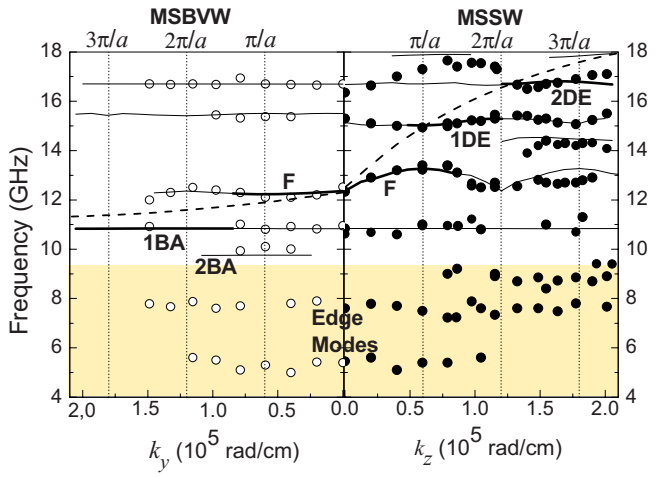

FIG. 5. (Color online) Collective mode dispersion for an applied field H_0=1.5 kOe measured in the MSSW (full circles) and MSBVW (open circles) configuration. Dots: experiment. Lines: simulation. Bold lines indicate the most intense response. The dashed lines are the dispersion of the DE mode and BA mode of the continuous film (from Fig. 2).

By comparing the calculation results with the BLS intensity spectra we see that as the value of k increases from the centre to the border of the first BZ (i.e. from $k=0$ to $k=k_{BZ}=\pi/a$) the most intense peak corresponds to the collective F mode. As the value of k increases, other modes become dominant. At $k=2.2\pi/a$, for example, the fundamental mode disappears from the set of the 20 most intense modes of the spectrum while the 2DE and the 2BA are the dominant modes in the MSSW and MSBVW configuration, respectively. For a detailed discussion of the dependence of the BLS cross section on the profile of collective modes, see Ref. 3.

Remarkably, in the MSSW configuration the F and the 1DE modes exhibit an oscillating behavior, whose span is about 1 and 0.5 GHz, respectively. This indicates that these modes are *traveling* waves of Bloch type. The dynamic dipolar interdot coupling is the origin of the capability of these modes to travel. As Bloch waves, these modes are characterized by a periodicity in the reciprocal space in the form of Brillouin zones whose width is determined by the pattern geometry. Note, that at the centre of the BZ ($k=0$) the calculated group velocity of the F mode $[v_g=d(2\pi\nu)/dk=1.97\ \mu\text{m/ns}]$ is smaller that the corresponding value for the continuous film $v_g=d(2\pi\nu)/dk=2.83\ \mu\text{m/ns}$, which represents the upper limit for the dispersion slope of collective modes on the periodically patterned sample.

Different from the case of F and 1DE modes, the other modes are practically dispersionless, i.e., their frequencies do not change as a function of the wave vector. Similar to the case of dipole-coupled stripes,[6] this behavior can be understood taking into account the fact that a spin-wave mode produces a dynamic dipole (stray) field whose strength is related to the spatial profile of the mode itself. In fact, the dynamic stray field has significant values only for the F and the 1DE modes while it dramatically decreases for the modes presenting several nodes.[33] This decrease in the stray field strength leads to a weaker dipolar coupling and consequently to the decrease in the width of the mode frequency band. The frequency minimum for the F mode is measured at the centre of the first Brillouin zone ($k=0$), where magnetization precession in all dots is in-phase while the maximum is reached at its edge ($k=k_{BZ}=\pi/a$) which corresponds to an antiphase precession of nearest neighbors dots in the direction of k. An opposite behavior has been observed for the 1DE mode, which exhibits the maximum and the minimum of the spin-wave frequency at the centre and at the edge of the first Brillouin zone, respectively. The evolution of the spin-wave frequency within the first BZ in the MSSW configuration, can be understood considering that for both the F and the 1DE mode, the dynamical coupling is dominated by the in-plane component (m_z) of the dynamical magnetization which is much larger than the out-of-plane one (m_x). Similarly to the case of the interacting wires, when the m_z component of a mode has the same direction at the adjacent edges of neighboring dots (at the centre and at the edge of the first BZ for the F and the 1 DE modes, respectively), the dipolar energy decreases, resulting in a decrease in the spin-wave frequency. When the m_z component of a mode has opposite direction at the adjacent edges of neighboring dots (at the edge and at the centre of the first BZ for the F and the 1 DE modes, respectively), the dipolar energy increases, inducing an increase in the spin-wave frequency.

In contrast with the above discussed behavior of the modes measured in the MSSW configuration, measurements in the MSBVW geometry do not show noticeable dispersion for any modes (Figs. 4 and 5, left side). There are two main reasons for this.

First of all, both the frequency bandwidth and the dispersion slope for collective modes of the periodically-patterned samples have upper limits given by the dispersion law for the unpatterned (continuous) film. In particular, for interdot distance $\Delta\to\infty$ the collective modes are dispersionless while for $\Delta=0$ one recovers the dispersion of the continuous film.[7,27] Now, the dispersion of BA modes in unpatterned metallic films is much smaller than the DE dispersion, as it can be inferred from the measured frequency dispersion for the reference continuous film of the same thickness and made in the same production cycle as the squared dot array (see Fig. 2). In this case the calculated group velocity for the F mode of the dots array and the backwardlike wave of the continuous film near to $k=0$ are almost equal $[v_g=d(2\pi\nu)/dk=-0.41\ \mu\text{m/ns}]$ and, as expected, are smaller than the measured value for the Voigt configuration (see also Fig. 5).

Second, because of the presence of edge domains where the internal field is strongly inhomogeneous, the separation of the areas of localization of the fundamental mode in neighboring dots is larger in the direction of the applied field than in the perpendicular direction. (i.e., the "effective" Δ is larger and the effective w is smaller). This results in a smaller dynamic dipole coupling of BA modes, detected in the MSBVW configuration.

Turn now to the low-frequency peaks (below about 10 GHz) in BLS spectra. Our calculations show that they correspond to modes localized at the edges of the dots, i.e., EMs confined in regions where the internal field is highly inhomogeneous.[21] As seen from Fig. 5, some of these peaks

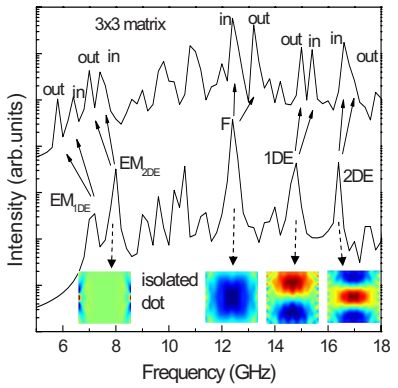

FIG. 6. (Color online) Power spectrum of magnetic excitations in an isolated single dot (lower spectrum) and in the central element of a 3×3 matrix of interacting dots calculated using the OOMMF micromagnetic code. The external field value is $H_0=1.5$ kOe. The arrows indicate the splitting of each of the labeled peaks of the isolated dot in a doublet of peaks with in-phase (in) or out-of-phase (out) oscillation in adjacent dots. The lower insets show the calculated spatial profiles of the dynamical magnetization for some of the principal modes of the isolated dot.

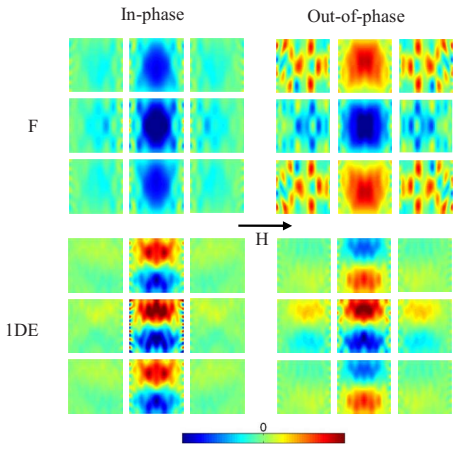

FIG. 7. (Color online) Calculated spatial profile of the dynamical magnetization of collective F and 1DE modes for a 3×3 matrix of interactive dots after perturbation of the central dot with a perpendicular field pulse. It is seen that the main interaction is between the central dot and those adjacent to it in the vertical direction, i.e., in the direction perpendicular to the applied field.

could be traced over a large interval of angles of laser light incidence in both MSSW and MSBVW configurations. In both cases no noticeable dispersion is seen. Unfortunately, it is generally difficult to accurately predict frequencies for edge modes in a simple model making use of approximation in Eq. (2), i.e., assuming a homogeneous magnetization within the dot. The reason is that their frequencies depend on the magnetic domains structure close to the elements edges (S and C states or flower state) which is strongly affected by material and edge defects and by the sample magnetization history. Moreover, for coupled resonances, the strength of dynamical coupling depends on the exact distance between the areas of their localization. For the above reasons, the theoretical calculation based on assumption of the uniform static magnetization, cannot yield realistic prediction concerning EM frequencies and spatial profiles of modes located below about 10 GHz (shadowed area in Fig. 5). One has to include the realistic profile for the static magnetization into the mode calculation. For instance, the static magnetization profile may be obtained from an OOMMF simulation, as it was done in Ref. 34, while calculating mode profiles for guided spin waves modes of magnetic stripes. However, there is a more straightforward approach which we will use in the next section.

B. Micromagnetic simulations

In order to verify the results delivered by the simple model discussed above and overcome its limitations in the analysis of edge modes we performed micromagnetic OOMMF simulations for a 3×3 matrix of dots, according to the procedure described in Sec. II. In particular, we calculated the power spectrum of spin excitations after the application of a perpendicular field pulse to the central dot of the matrix. In Fig. 6 we show a comparison between the power spectra for the isolated squared dot and for the central element of a 3×3 matrix of dots. From this figure it is evident that some peaks, corresponding to the principal modes, undergo a splitting. For the F, 1DE, and 2DE modes this is indicated by the arrows in the figure.

The spatial profiles corresponding to each peak of the doublets relative to the F and 1DE modes of the 3×3 array are shown in Fig. 7. Note that the in-phase and the out-of-phase collective modes correspond to the centre and to the edge of the first BZ of the continuous array, respectively. From a simple inspection of such profiles it is evident that starting from the central dot, where the field pulse is applied, the strength of the coupling is much more intense in the direction perpendicular to the static field compared to the parallel one. This is in agreement with the above discussed finding that the DE-like modes are more affected by the coupling and exhibit a stronger dispersive character than the BA-like ones.

Furthermore, the peak at low (high) frequency in the doublets resulting from either the F or the 2DE mode, indicated by the arrows in Fig. 6, corresponds to an in-phase (out-of-phase) spin precession in adjacent dots along the direction perpendicular to the field. The opposite happens for the doublet relative to the 1DE mode, confirming the different slopes of their dispersion curves in Fig. 5. The reason for this difference in the behavior can be understood looking at the sign of the dynamical magnetization at the borders of adjacent dots along the vertical direction in Fig. 7. For the F mode the same sign is achieved for the in-phase precession while for the 1DE mode the oscillation at the borders of adjacent dots have the same sign for out-of-phase precession. The frequency difference between the in-phase and out-of-phase precessions of the F (1DE) mode is 0.8 GHz (0.4 GHz) which is in very good agreement with the result of the Fourier space approach described in Sec. III and satisfactorily reproduces the measured width of the frequency band for the above mentioned modes.

In the final part of our paper, let us discuss the properties of EMs analyzing the results of micromagnetic simulations.[35]

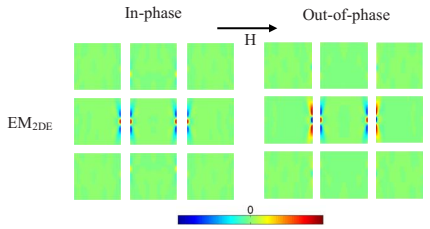

FIG. 8. (Color online) Calculated spatial profile of the collective EM_{2DE} mode for a 3×3 matrix of interactive dots, after perturbation of the central dot with a perpendicular field pulse. It is evident that the main interaction is between the borders of the central dot and those adjacent to it in the horizontal direction, i.e., in the direction parallel to the applied field. The calculated frequency different between the "in-phase" (left panel) and the "out-of-phase" (right panel) mode is about 0.4 GHz, as seen also in Fig. 6.

As in the case of the high-frequency modes, there is a splitting of the EMs peaks in the calculated power spectra (for example, modes EM_{1DE} and EM_{2DE} indicated in Fig. 6), confirming the influence of the dipolar coupling. However, we note that for EMs the effect is opposite to what was previously observed for the F or the DE modes: the higher frequency mode is now characterized by in-phase magnetization precession at the neighboring edges of adjacent dots while the lower frequency one by antiphase precession (see Fig. 8, where the EM_{2DE} mode is shown as an example). This difference can be explained taking into account the intensity of the dipolar field produced by the dynamic magnetization. For the EMs the stray field of the m_z component is small. It exists only because of dot confinement along z and would vanish if the dots merged into continuous stripes along z. On the contrary, the dipole field induced by m_x is large (its limiting value $-4\pi m_x$ is obtained for the vanishing gap in the x direction). It is contra-aligned to the dynamic magnetization vector which induces this field. Thus for the antiphase precession at the adjacent edges of a two dots the stray field from the neighbor is coaligned with the direction of the own m_x of the dot. In this way the dipole energy is minimized and the frequency is smaller than for the edge modes for uncoupled dots. On the contrary, for the in-phase precession the contribution to the total dipole field from the closest neighbor is antialigned to m_x in each dot so the total dipole energy is maximized and the mode frequency is larger than for the antiphase precession. This splitting between an in-phase and an out-of-phase precession of EMs in adjacent dots resembles the appearance of "acoustic" and "optical" modes in a magnetic bilayer separated by a nonmagnetic interlayer.

It is important to remark, however, that the nature of the dipole interactions underlying the frequency splitting evidenced by the arrows in Fig. 6 differs for DE or BA modes and EM. For the DE and BA modes the dipolar coupling induces the formation of true collective modes which propagates through the lattice and the splitted peaks obtained in the OOMMF simulation (Fig. 6) indicate the approximate positions for the upper and lower limits for their frequency bands. For EMs, instead, the magnetization oscillations localized at the edges of two adjacent dots couple but the oscillations localized at the opposite edges of the same dot are not phase correlated. This results in no dispersion for the EM modes in the MSBVW configuration; the modes of the doublets have a localized nature and are characterized by discrete frequencies. Unfortunately, this splitting of the EDs has not been experimentally observed. This is probably due to that fact this splitting is relatively small and strongly affected by the details of edge domains. Therefore in the real sample the frequency difference between the modes of a doublet can be strongly reduced by the presence of the edge defects.

As for the MSSW configuration, strictly speaking, the EMs form collective excitations. However, their dispersion is almost negligible, reflecting the weak dynamical interdot coupling and the rather localized character of these modes. This is evident from inspection of Fig. 8, where it is seen that the dots which are over and above the central one are practically unaffected by the excitation of the EM in the central dot.

V. CONCLUSIONS

In this paper we have exploited BLS to study the thermally excited spin wave modes in a 2D magnonic crystal consisting of interacting nanodots. This technique allowed us to study dynamic magnetic dipole coupling of the elements separately from the static magnetic coupling which is always present in closely packed 2D arrays of magnetic nanostructures. Measurements recorded as a function of the magnitude and the direction of the exchanged wave vector enabled us to give experimental evidence of traveling collective modes, whose frequency dispersion is characterized by a full magnonic gap. The frequency dispersion for the modes has been calculated by numerically solving eigenvalue/eigenfunction problem for a band matrix which originates from the linearized Landau-Lifschitz magnetic torque equation. This permitted us to quantitatively explain the observed frequency dispersion of the modes in terms of dynamical dipolar coupling and to discuss its influence on different classes of eigenmodes. In addition, the spatial profiles of the modes have been mapped out by micromagnetic simulations on a limited array (3×3) of dots, confirming the main findings achieved by the analytical model.

Our main finding is a considerable anisotropy of dynamical coupling for propagating collective modes. The modes propagating perpendicular to the applied magnetic field may acquire considerable group velocities but the modes with Bloch wave vectors along the field are characterized by negligible velocities. An important contribution to this anisotropy is the static demagnetizing field which effectively increases the interdot separation in the direction of the applied field.

ACKNOWLEDGMENTS

The research leading to these results has received funding from the European Community's Seventh Framework Programme (FP7/2007-2013) under Grant No. 228673 (MAGNONICS). Support by Australian Research Council and by Ministero Italiano dell'Università e della Ricerca, under PRIN research project are kindly acknowledged.

[1] S. Neusser and D. Grundler, Adv. Mater. **21**, 2927 (2009).
[2] V. V. Kruglyak, S. O. Demokritov, and D. Grundler, J. Phys. D: Appl. Phys. **43**, 264001 (2010).
[3] L. Giovannini, F. Montoncello, and F. Nizzoli, Phys. Rev. B **75**, 024416 (2007).
[4] P. Politi and M. G. Pini, Phys. Rev. B **66**, 214414 (2002).
[5] Z. K. Wang, V. L. Zhang, H. S. Lim, S. C. Ng, M. H. Kuok, S. Jain, and A. O. Adeyeye, Appl. Phys. Lett. **94**, 083112 (2009).
[6] G. Gubbiotti, S. Tacchi, G. Carlotti, P. Vavassori, N. Singh, S. Goolaup, A. O. Adeyeye, A. Stashkevich, and M. Kostylev, Phys. Rev. B **72**, 224413 (2005).
[7] M. Kostylev, P. Schrader, R. L. Stamps, G. Gubbiotti, G. Carlotti, A. O. Adeyeye, S. Goolaup, and N. Singh, Appl. Phys. Lett. **92**, 132504 (2008); G. Gubbiotti, S. Tacchi, G. Carlotti, N. Singh, S. Goolaup, A. O. Adeyeye, and M. Kostylev, *ibid.* **90**, 092503 (2007).
[8] M. P. Kostylev, A. A. Stashkevich, and N. A. Sergeeva, Phys. Rev. B **69**, 064408 (2004).
[9] K. Rivkin, W. Saslow, V. Chandrasehkhar, L. E. De Long, and J. B. Ketterson, Phys. Rev. B **75**, 174408 (2007).
[10] G. Gubbiotti, M. Madami, S. Tacchi, G. Carlotti and T. Okuno, J. Appl. Phys. **99**, 08C701 (2006).
[11] J. Jorzick, S. O. Demokritov, B. Hillebrands, B. Bartenlian, C. Chappert, D. Decanini, F. Rousseaux, and E. Cambril, Appl. Phys. Lett. **75**, 3859 (1999).
[12] Ch. Mathieu, C. Hartmann, M. Bauer, O. Büttner, S. Riedling, B. Roos, S. O. Demokritov, B. Hillebrands, B. Bartenlian, C. Chappert, D. Decanini, F. Rousseaux, E. Cambrill, A. Müller, B. Hoffmann, and U. Hartmann, Appl. Phys. Lett. **70**, 2912 (1997).
[13] Z. K. Wang, M. H. Kuok, S. C. Ng, D. J. Lockwood, M. G. Cottam, K. Nielsch, R. B. Wehrspohn, and U. Gösele, Phys. Rev. Lett. **89**, 027201 (2002).
[14] V. V. Kruglyak, P. S. Keatley, R. J. Hicken, J. R. Childress, and J. A. Katine, J. Appl. Phys. **99**, 08F306 (2006); P. S. Keatley, V. V. Kruglyak, A. Neudert, E. A. Galaktionov, R. J. Hicken, J. R. Childress, and J. A. Katine, Phys. Rev. B **78**, 214412 (2008).
[15] V. V. Kruglyak, P. S. Keatley, A. Neudert, R. J. Hicken, J. R. Childress, and J. A. Katine, Phys. Rev. Lett. **104**, 027201 (2010)
[16] G. N. Kakazei, Yu. G. Pogorelov, M. D. Costa, T. Mewes, P. E. Wigen, P. C. Hammel, V. O. Golub, T. Okuno, and V. Novosad, Phys. Rev. B **74**, 060406(R) (2006).
[17] M. Donahue and D. G. Porter, OOMMF User's guide, Version 1.0, Interagency Report NISTIR 6376, NIST, Gaithersburg, MD, 1999, http://math.nist.gov/oommf
[18] R. D. McMichael and M. D. Stiles, J. Appl. Phys. **97**, 10J901 (2005).
[19] In order to efficiently excite modes with different spatial symmetries we apply to the central dot of the array a field pulse perpendicular to the sample plane. It is obtained as the sum of an uniform pulse and a pulse with an odd symmetry with respect to the direction defined by the in-plane external field H_0.
[20] N. I. Polushkin, Phys. Rev. B **77**, 180401(R) (2008).
[21] C. Bayer, J. Jorzick, S. O. Demokritov, A. N. Slavin, K. Y. Guslienko, D. V. Berkov, N. L. Gorn, M. P. Kostylev, and B. Hillebrands, Top. Appl. Phys. **101**, 57 (2006), and references therein.
[22] M. P. Kostylev, G. Gubbiotti, J.-G. Hu, G. Carlotti, T. Ono, and R. L. Stamps, Phys. Rev. B **76**, 054422 (2007).
[23] K. Yu. Guslienko, S. O. Demokritov, B. Hillebrands, and A. N. Slavin, Phys. Rev. B **66**, 132402 (2002).
[24] B. A. Kalinikos, IEE Proc., Part H: Microwaves, Opt. Antennas **127**, 4 (1980).
[25] M. P. Kostylev, A. A. Serga, T. Schneider, T. Neumann, B. Leven, B. Hillebrands, and R. L. Stamps, Phys. Rev. B **76**, 184419 (2007).
[26] M. Kostylev and A. Stashkevich (unpublished).
[27] M. P. Kostylev and N. A. Sergeeva, in *Magnetic Properties of Laterally Confined Nanometric Structures*, edited by G. Gubbiotti (Transworld Research Network, Kerala, India, 2006), pp. 183–207.
[28] L. Giovannini, F. Montoncello, F. Nizzoli, G. Gubbiotti, G. Carlotti, T. Okuno, T. Shinjo, and M. Grimsditch, Phys. Rev. B **70**, 172404 (2004).
[29] C. Mathieu, J. Jorzick, A. Frank, S. O. Demokritov, A. N. Slavin, B. Hillebrands, B. Bartenlian, C. Chappert, D. Decanini, F. Rousseaux, and E. Cambril, Phys. Rev. Lett. **81**, 3968 (1998).
[30] C. Bayer, J. Jorzick, B. Hillebrands, S. O. Demokritov, R. Kouba, R. Bozinoski, A. N. Slavin, K. Guslienko, D. Berkov, N. Gorn, and M. P. Kostylev, Phys. Rev. B **72**, 064427 (2005).
[31] M. Madami, S. Tacchi, G. Gubbiotti, G. Carlotti, F. Montoncello, G. Capuzzo, L. Giovannini, F. Nizzoli, H. Tanigawa, and T. Ono, IEEE Trans. Magn. **46**, 199 (2010).
[32] M. P. Kostylev and A. A. Stashkevich, Phys. Rev. B **81**, 054418 (2010).
[33] G. Gubbiotti, S. Tacchi, M. Madami, G. Carlotti, A. Adeyeye, and M. Kostylev, J. Phys. D: Appl. Phys. **43**, 264003 (2010).
[34] A. V. Chumak, P. Pirro, A. A. Serga, M. P. Kostylev, R. L. Stamps, H. Schultheiss, K. Vogt, S. J. Hermsdoerfer, B. Laegel, P. A. Beck, and B. Hillebrands, Appl. Phys. Lett. **95**, 262508 (2009).
[35] In the case of edge modes the choice of different ground states for the dynamic simulation (i.e., C and S state or flower state) could result in quite different outcomes for the calculated frequency and spatial profile. The mode profiles and power spectra showed in this work have been all obtained using a flower ground state, both for the isolated dot and the 3×3 array of squares.